

# Heavy Quark Fragmentation in Deep Inelastic Scattering

S. Kretzer and I. Schienbein

Institut für Physik, Universität Dortmund  
D-44221 Dortmund, Germany

## Abstract

We perform an analysis of semi-inclusive production of charm (D-mesons) in neutral current (NC) and charged current (CC) deep inelastic scattering (DIS) at full  $\mathcal{O}(\alpha_s^1)$ . Our calculation is based on the heavy quark scheme developed by Aivazis, Collins, Olness and Tung (ACOT) where we include an  $\mathcal{O}(\alpha_s^1)$  calculation of quark scattering contributions for general masses and couplings. We review the relevant massive formulae and subtraction terms and discuss their massless limits. We show how the charm fragmentation function can be measured in CC DIS and we investigate whether the charm production dynamics may be tested in NC DIS. We also discuss finite initial state quark mass effects in CC and NC DIS.

# 1 Introduction

In a recent paper [1] we have analyzed heavy quark initiated contributions to fully inclusive deep inelastic (DI) structure functions. Towards lower values of the Bjorken variable  $x$ , heavy (charm) quarks are produced in about 20 % of the neutral current (NC) [2, 3] and charged current (CC) [4] deep inelastic events in lepton-nucleon collisions. Therefore in this kinematical range, heavy quark events contribute an important component to the fully inclusive DI structure functions of the nucleon. However, due to acceptance losses this component can usually not be measured directly by inclusively tagging on charm events and more differential observables have to be considered like  $E_D$  [5, 6, 7],  $p_T$  or  $\eta$  [2, 3] distributions, where  $E_D$ ,  $p_T$  and  $\eta$  are the energy, transverse momentum and pseudorapidity of the charmed hadron produced, i.e. mainly of a  $D^{(*)}$  meson. In this article we consider  $E_D$  spectra represented by the usual scaling variable  $z$  defined below. Within DIS the charmed hadron energy spectrum is the distribution which is most sensitive to the charm fragmentation process and may give complementary information to one hadron inclusive  $e^+e^-$  annihilation which is usually chosen to define fragmentation functions (FF's) [8, 9]. A well understanding of charm fragmentation is essential for any charm observable, e.g. the normalization of  $p_T$  and  $\eta$  distributions in photoproduction is substantially influenced by the hardness of the FF [10, 11]. The  $z$  distribution of charm fragments is directly measured in CC neutrino production [5, 6, 7, 12] and may give insight into details of the charm production dynamics in NC electroproduction. It has e.g. been shown in [2, 3], that the energy spectrum of  $D^{(*)}$ -mesons produced at the  $eP$ -collider HERA may be able to discriminate between intrinsic and extrinsic production of charm quarks.

Intrinsic heavy quark densities may arise due to a nonperturbative component of the nucleon wave function [13] or due to a perturbative resummation [14, 15, 16, 17] of large quasi-collinear logs  $[\ln(Q^2/m^2)]$ ;  $Q$  and  $m$  being the virtuality of the mediated gauge boson and the heavy quark mass, respectively] arising at any order in fixed order extrinsic production (or fixed order perturbation theory: FOPT). Here we will only consider the

latter possibility for inducing an intrinsic charm density  $c(x, Q^2)$  which is concentrated at small  $x$  and we will ignore nonperturbative components which are expected to be located at large  $x$  [13]. Technically the resummation of large perturbative logs proceeds through calculating the boundary conditions for a transformation of the factorization scheme [18, 17, 19], which is switched from  $n_f$  to  $n_f+1$  active, massless flavors, canonically at  $Q^2 = m^2$ . For fully inclusive DIS the Kinoshita-Lee-Nauenberg theorem confines all quasi-collinear logs to the initial state such that they may be absorbed into  $c(x, Q^2)$ . For semi-inclusive DIS (SI DIS) also final state collinearities arise which are resummed in perturbative fragmentation functions  $D_i^c(z, Q^2)$  (parton  $i$  decaying into charm quark  $c$ ) along the lines of [19, 10]. The scale dependence of  $c(x, Q^2)$  and  $D_i^c(z, Q^2)$  is governed by massless renormalization group (RG) evolution.

Besides this *zero mass variable flavor number scheme*, where mass effects are only taken care of by the boundary conditions for  $c(x, Q^2)$  and  $D_i^c(z, Q^2)$ , variable flavor number schemes have been formulated [14, 15, 16, 17], which aim at resumming the quasi-collinear logs as outlined above while also keeping power suppressed terms of  $\mathcal{O}[(m^2/Q^2)^k]$  in the perturbative coefficient functions. Our reference scheme for this type of schemes will be the one developed by Aivazis, Collins, Olness and Tung (ACOT) [20, 14]. In the ACOT scheme full dependence on the heavy quark mass is kept in graphs containing heavy quark lines. This gives rise to the above mentioned quasi-collinear logs and to the power suppressed terms. While the latter are regarded as mass corrections to the massless, dimensionally regularized, standard coefficient functions (e.g. in the  $\overline{\text{MS}}$  scheme), the former are removed numerically by subtraction terms, which are obtained from the small mass limit of the massive coefficient functions.

The outline of our paper will be the following: In section 2 we will shortly overview the relevant formulae for SI DIS for general masses and couplings including quark scattering (QS) and boson gluon fusion (GF) contributions up to  $\mathcal{O}(\alpha_s^1)$ . We will thereby present our ACOT based calculation for the  $QS^{(1)1}$  component of SI structure functions. In section

---

<sup>1</sup> Bracketed upper indices count powers of  $\alpha_s$ .

3 we will analyze the charm fragmentation function in CC and NC DIS. In section 4 we draw our conclusions and some uncomfortably long formulae are relegated to an appendix.

## 2 Semi-Inclusive Heavy Quark Structure Functions

This section presents the relevant formulae for one (heavy flavored) hadron inclusive DIS structure functions. The contributions from scattering events on massive quarks are given up to  $\mathcal{O}(\alpha_s^1)$  in section 2.1 and GF contributions are briefly recalled in section 2.2. Section 2.3 presents all subtraction terms which render the structure functions infrared safe and includes a discussion of these terms.

### 2.1 Scattering on Massive Quarks

We consider DIS of the virtual Boson  $B^*$  with momentum  $q$  on the quark  $Q_1$  with mass  $m_1$  and momentum  $p_1$  producing the quark  $Q_2$  with mass  $m_2$  and momentum  $p_2$ . The latter fragments into a heavy quark flavored hadron  $H_{Q_2}$ , e.g. a  $|Q_2 \bar{q}_l\rangle$  meson,  $q_l$  being any light quark. Phenomenologically most prominent are of course charm quarks fragmenting into  $D^{(*)}$ -mesons which are the lightest heavy flavored hadrons.

We will strictly take over the formulae and notations of our inclusive analysis in [1] whenever possible and merely extend them for SI DIS considered here. In particular we take over the definition of the structure functions  $\mathcal{F}_i$  given in terms of the usual experimental structure functions  $F_i$  in Eq. (7) in [1], i.e.

$$\begin{aligned}\mathcal{F}_1 &= \frac{2\Delta}{S_+ \Sigma_{++} - 2m_1 m_2 S_-} F_1 \\ \mathcal{F}_2 &= \frac{2Q^2}{S_+ \Delta} \frac{1}{2x} F_2 \\ \mathcal{F}_3 &= \frac{1}{2R_+} F_3 \quad ,\end{aligned}\tag{1}$$

with

$$\Sigma_{\pm\pm} \equiv Q^2 \pm m_2^2 \pm m_1^2 \quad .\tag{2}$$

In Eq. (1) we use the shorthand  $\Delta \equiv \Delta[m_1^2, m_2^2, -Q^2]$ , where the usual triangle function is defined by

$$\Delta[a, b, c] = \sqrt{a^2 + b^2 + c^2 - 2(ab + bc + ca)} \quad . \quad (3)$$

The vector ( $V$ ) and axial vector ( $A$ ) couplings of the  $\bar{Q}_2 \gamma_\mu (V - A \gamma_5) Q_1$  quark current enter via the following combinations:

$$\begin{aligned} S_\pm &= VV' \pm AA' \\ R_\pm &= (VA' \pm V'A)/2 \end{aligned} \quad (4)$$

where  $V, A \equiv V', A'$  in the case of pure  $B$  scattering and  $V, A \neq V', A'$  in the case of  $B, B'$  interference (e.g.  $\gamma, Z^0$  interference in the standard model).

Since we want to investigate the energy spectrum of charm fragments, we introduce the Lorentz-invariant  $z \equiv p_{H_{Q_2}} \cdot p_N / q \cdot p_N$  which reduces to the energy  $E_{H_{Q_2}}$  scaled to its maximal value  $\nu = q_0$  in the target rest frame. Therefore in contrast to Eq. (A4) in [1] we do not integrate the tensor  $\hat{\omega}^{\mu\nu}$  over the full partonic phase space but keep it differential in the corresponding partonic variable  $z' \equiv p_2 \cdot p_1 / q \cdot p_1$  or the mass corrected variable  $\hat{z}$  which is defined below. In order to obtain hadronic observables we have to extend the ansatz of Eq. (17) in [20] such that it includes a nonperturbative hadronization function  $D_{Q_2}$ . In the limit of vanishing masses the massless parton model expressions have to be recovered. Our ansatz will be

$$W^{\mu\nu} = \int \frac{d\xi}{\xi} \frac{d\zeta}{\zeta} Q_1(\xi, \mu^2) D_{Q_2}(\zeta, [\mu^2]) \hat{\omega}^{\mu\nu}|_{\{p_1^+ = \xi P^+; z = \zeta \hat{z}\}} \quad , \quad (5)$$

where  $\mu$  is the factorization scale,  $\hat{z} = z'/z'_{LO}$  with  $z'_{LO} = \Sigma_{++}/\Sigma_{+-}$  and  $v^+ \equiv (v^0 + v^3)/\sqrt{2}$  for a general vector  $v$ .  $W^{\mu\nu}$  is the usual hadronic tensor and  $\hat{\omega}^{\mu\nu}$  is its partonic analogue. Eq. (5) defines the fragmentation function  $D_{Q_2}$  to be a multiplicative factor multiplying inclusive structure functions at LO/Born accuracy, i.e.

$$\mathcal{F}_{i=1,2,3}^{QS(0)}(x, z, Q^2) = \mathcal{F}_{i=1,2,3}^{QS(0)}(x, Q^2) D_{Q_2}(z, [Q^2]) \quad , \quad (6)$$

where the  $\mathcal{F}_{i=1,2,3}^{QS(0)}(x, Q^2)$  are defined and given in [1]. The scale dependence of  $D_{Q_2}$  is bracketed here and in the following because it is optional; a more detailed discussion on

this point will be given at the end of section 2.3. We do not construct our ansatz in Eq. (5) for the convolution of the fragmentation function along light front components for the outgoing particles which would only be Lorentz-invariant for boosts along a specified axis. Since the final state of DIS is spread over the entire solid angle it has no preferred axis as defined for the initial state by the beam direction of collider experiments. Note that eq. (5) is in agreement with usual factorized expressions for massless initial state quanta, e.g. in [21], since there  $m_1 = 0$  such that  $z'_{LO} = 1$ .

Up to  $\mathcal{O}(\alpha_s^1)$  the hadronic structure functions for scattering on a heavy quark read

$$\begin{aligned} \hat{\mathcal{F}}_{i=1,2,3}^{QS(0+1)}(x, z, Q^2, \mu^2) &= Q_1(\chi, \mu^2) D_{Q_2}(z, [\mu^2]) + \frac{\alpha_s(\mu^2)}{2\pi} \int_{\chi}^1 \frac{d\xi'}{\xi'} \int_z^1 \frac{d\hat{z}}{\hat{z}} \\ &\times \left[ Q_1\left(\frac{\chi}{\xi'}, \mu^2\right) \hat{H}_i^q(\xi', z', \mu^2) \Theta_q \right] D_{Q_2}\left(\frac{z}{\hat{z}}, [\mu^2]\right) , \end{aligned} \quad (7)$$

with [20, 1]

$$\chi = \frac{x}{2Q^2} (\Sigma_{+-} + \Delta) . \quad (8)$$

In Eq. (7) and throughout this paper we set the renormalization scale equal to the factorization scale. The kinematical boundaries of the phase space in Eq. (7) are introduced by the theta function cut  $\Theta_q$ . In the massless limit  $\Theta_q \rightarrow 1$ . The precise arguments of  $\Theta_q$  are set by the kinematical requirement

$$z'_{min} < z' < z'_{max} , \quad (9)$$

with

$$z'_{min} = \frac{\pm \Delta[\hat{s}, m_1^2, -Q^2](\hat{s} - m_2^2) + (Q^2 + m_1^2 + \hat{s})(\hat{s} + m_2^2)}{2\hat{s}(\hat{s} - m_1^2 + Q^2)} ,$$

where  $\hat{s} = (p_1 + q)^2$ . Note that Eq. (9) also poses an implicit constraint on  $\xi'$  via  $z'_{min} < z'_{max}$ .

The  $\hat{H}_i^q$  for nonzero masses are obtained in exactly the same way as outlined for fully inclusive structure functions in [1] if the partonic phase space is not fully integrated over. They are given by

$$\hat{H}_i^q(\xi', z') = C_F \left[ (S_i + V_i) \delta(1 - \xi') \delta(1 - \hat{z}) \right]$$

$$+ \frac{1 - \xi'}{(1 - \xi')_+} \frac{z'_{LO}}{8} \frac{\hat{s}_1 + \Sigma_{+-}}{\Delta'} N_i^{-1} \hat{f}_i^Q(\hat{s}_1, \hat{t}_1) \Big] \quad (10)$$

with the normalization factors

$$N_1 = \frac{S_+ \Sigma_{++} - 2m_1 m_2 S_-}{2\Delta}, \quad N_2 = \frac{2S_+ \Delta}{\Delta'}, \quad N_3 = \frac{2R_+}{\Delta'},$$

and the mandelstam variables

$$\begin{aligned} \hat{s}_1(\xi') &\equiv (p_1 + q)^2 - m_2^2 \\ &= \frac{1 - \xi'}{2\xi'} [(\Delta - \Sigma_{+-})\xi' + \Delta + \Sigma_{+-}] \\ \hat{t}_1(\xi', z') &\equiv (p_1 - p_3)^2 - m_1^2 \\ &= [\hat{s}_1(\xi') + \Sigma_{+-}](z' - z'_0) \end{aligned}$$

where  $z'_0 = \frac{\hat{s}_1 + \Sigma_{++}}{\hat{s}_1 + \Sigma_{+-}}$  is the would-be pole of the  $\hat{t}$ -channel propagator and we use  $\Delta' \equiv \Delta[\hat{s}, m_1^2, -Q^2]$ .  $S_i$  and  $V_i$  are the soft real and virtual contribution to  $\hat{H}_i^q$ , respectively. They can be found in appendix C of [1] whereas the  $\hat{f}_i^Q(\hat{s}_1, \hat{t}_1)$  are listed in appendix A of this paper. In the massless limit the  $\hat{H}_i^q$  reduce to the  $\overline{\text{MS}}$  coefficient functions in [8, 22] up to some divergent subtraction terms which we will specify in section 2.3.

## 2.2 Gluon Fusion Contributions at $\mathcal{O}(\alpha_s^1)$

The semi-inclusive coefficient functions for GF production of massive quarks have been obtained for general masses and couplings in [21] and are only briefly reviewed here for completeness. They are given by

$$\begin{aligned} \hat{F}_{1,3}^{GF}(x, z, Q^2, \mu^2) &= \int_{ax}^1 \frac{dx'}{x'} \int_z^1 \frac{d\zeta}{\zeta} g(x', \mu^2) f_{1,3}\left(\frac{x}{x'}, \zeta, Q^2\right) D_{Q_2}\left(\frac{z}{\zeta}, [\mu^2]\right) \Theta_g \\ \hat{F}_2^{GF}(x, z, Q^2, \mu^2) &= \int_{ax}^1 \frac{dx'}{x'} \int_z^1 \frac{d\zeta}{\zeta} x' g(x', \mu^2) f_2\left(\frac{x}{x'}, \zeta, Q^2\right) D_{Q_2}\left(\frac{z}{\zeta}, [\mu^2]\right) \Theta_g \end{aligned} \quad (11)$$

with  $ax = [1 + (m_1 + m_2)^2/Q^2]x$ . The  $\Theta_g$  cut guarantees that  $\zeta_{min} < \zeta < \zeta_{max}$  where  $\zeta_{min, max}$  are given in Eq. (3) of [21]. Similarly to Eq. (9)  $\zeta_{min} < \zeta_{max}$  may also constrain the phase space available for the  $x'$  integration.

## 2.3 Subtraction Terms

It requires three  $\overline{\text{MS}}$  subtraction terms to render the double convolutions in Eqs. (7), (11) infrared safe:

$$\begin{aligned} \mathcal{F}_i^{SUB_q}(x, z, Q^2, \mu^2) &= \frac{\alpha_s(\mu^2)}{2\pi} C_F \int_{\chi}^1 \frac{d\xi'}{\xi'} \left[ \frac{1 + \xi'^2}{1 - \xi'} \left( \ln \frac{\mu^2}{m_1^2} - 1 - 2 \ln(1 - \xi') \right) \right]_+ \\ &\times Q_1 \left( \frac{\chi}{\xi'}, \mu^2 \right) D_{Q_2}(z, [\mu^2]) \end{aligned} \quad (12)$$

$$\mathcal{F}_i^{SUB_g}(x, z, Q^2, \mu^2) = D_{Q_2}(z, [\mu^2]) \frac{\alpha_s(\mu^2)}{2\pi} \ln \frac{\mu^2}{m_1^2} \int_{\chi}^1 \frac{d\xi'}{\xi'} P_{qg}^{(0)}(\xi') g \left( \frac{\chi}{\xi'}, \mu^2 \right) \quad (13)$$

$$\begin{aligned} \mathcal{F}_i^{SUB_D}(x, z, Q^2, \mu^2) &= \frac{\alpha_s(\mu^2)}{2\pi} C_F \int_z^1 \frac{dz'}{z'} \left[ \frac{1 + z'^2}{1 - z'} \left( \ln \frac{\mu^2}{m_2^2} - 1 - 2 \ln(1 - z') \right) \right]_+ \\ &\times D_{Q_2} \left( \frac{z}{z'}, \mu^2 \right) Q_1(\chi, \mu^2) \quad , \end{aligned} \quad (14)$$

where  $P_{qg}^{(0)}(\xi') = 1/2 [\xi'^2 + (1 - \xi')^2]$ . Note that  $SUB_g$  in Eq. (13) differs slightly from Eq. (6) in [21] because we are allowing for a nonzero initial state parton mass  $m_1$  here which we did not in [21].

The subtraction terms define the running of the initial state quark density ( $SUB_q$ ,  $SUB_g$ ) and the final state fragmentation function ( $SUB_D$ ) in the massless limit. They remove collinear logarithms and scheme defining finite terms from the convolutions in Eqs. (7), (11) and they are constructed such that the massless  $\overline{\text{MS}}$  results of [8, 22] are recovered in the limit

$$\lim_{m_{1,2} \rightarrow 0} \left[ \hat{\mathcal{F}}_i^{QS^{(0+1)}+GF}(x, z, Q^2, \mu^2) - \mathcal{F}_i^{SUB_q+SUB_g+SUB_D}(x, z, Q^2, \mu^2) \right] = \mathcal{F}_i^{(1),\overline{\text{MS}}}(x, z, Q^2) \quad , \quad (15)$$

where  $SUB_q$  and  $SUB_D$  regularize  $\hat{\mathcal{F}}_i^{QS^{(0+1)}}$  whereas  $SUB_g$  regularizes  $\hat{\mathcal{F}}_i^{GF}$ . Contrary to the fully inclusive  $SUB_g$  term in Eq. (16) of [1] there is no need to include an additional  $\sim \ln(\mu^2/m_2^2)$  subtraction in Eq. (13) because the  $\zeta^{-1} \hat{u}$ -channel singularity of the massless limit of  $GF^{(1)}$  is located at  $\zeta = 0$  and is outside the integration volume of Eq. (11). If only initial state subtractions, i.e.  $SUB_q$  and  $SUB_g$ , are considered and final state



subtractions, i.e.  $SUB_D$ , are not performed one reproduces, in the limit  $m_1 \rightarrow 0$  the results in [12] for producing a heavy quark from a light quark. Note that in this case the fragmentation function  $D_{Q_2}$  should be taken scale-*independent*, say of the Peterson form [23]. In the limit where also the final state quark mass  $m_2$  approaches zero and the final state subtraction term  $SUB_D$  is subtracted from the results in [12] the massless quark results in [8, 22] are obtained and a running of  $D_{Q_2}$  is induced via a RG resummation of final state collinear logs as formulated for one hadron inclusive  $e^+e^-$  annihilation in [19, 10].

Apart from removing the long distance physics from the coefficient functions the subtraction terms set the boundary conditions for the intrinsic heavy quark density  $Q_1$  [18] and the perturbative part of the heavy quark fragmentation function  $D_{Q_2}$  [19]:

$$Q_1(x, Q_0^2) = \frac{\alpha_s(Q_0^2)}{2\pi} \ln \frac{Q_0^2}{m_1^2} \int_x^1 \frac{d\xi}{\xi} P_{qg}^{(0)}(\xi) g\left(\frac{x}{\xi}, Q_0^2\right) \quad (16)$$

$$D_{Q_2}(z, \tilde{Q}_0^2) = \frac{\alpha_s(\tilde{Q}_0^2)}{2\pi} C_F \int_z^1 \frac{dz'}{z'} \left[ \frac{1+z'^2}{1-z'} \left( \ln \frac{\tilde{Q}_0^2}{m_2^2} - 1 - 2 \ln(1-z') \right) \right]_+ D_{Q_2}\left(\frac{z}{z'}\right) \quad (17)$$

where  $Q_0, \tilde{Q}_0$  are the transition scales at which the factorization scheme is switched from  $n_f$  to  $n_f+1, n_f+2$  active flavors, respectively (assuming here for simplicity that  $m_1 < m_2$ ; a generalization to  $m_1 \geq m_2$  is straightforward). For general  $Q_0$  also the gluon density and  $\alpha_s$  undergo a scheme transformation. Here we omit the corresponding formulae which can be found in [18, 17] since they are not needed in our analysis. Canonically  $Q_0$  is set equal to the heavy quark mass  $m_1$  which guarantees [18] up to two loops a continuous evolution of  $\alpha_s$  and the light parton densities across  $Q_0$ . All available heavy quark densities are generated using  $Q_0 = m_1$  and we will therefore follow this choice here although a variation of  $Q_0$  might substantially influence the heavy quark results even far above the threshold [25]. Note that at three loops a continuous evolution across  $Q_0$  can no longer be achieved, neither for the parton distributions [17] nor for  $\alpha_s$  [26]. Analogously to  $Q_0 = m_1$  we use  $\tilde{Q}_0 = m_2$  throughout. In Eq. (17) we have made the distinction between the scale dependent FF  $D_{Q_2}(z, \tilde{Q}_0^2)$  and the scale independent FF  $D_{Q_2}(z)$  explicit. Following the

terminology in [19, 10] the latter corresponds to the nonperturbative part of the former and describes the hadronization process at the end of the parton shower which is described perturbatively by the massless RG evolution. Alternatively,  $D_{Q_2}(z)$  corresponds to a scale-independent FF within FOPT where no collinear resummations are performed. These two points of view may induce a scheme dependence if  $D_{Q_2}(z)$  is fitted to data. In principle, the massless evolution equations generate nonzero FF's also for light partons to decay into heavy flavored hadrons. These light $\rightarrow$ heavy contributions are important at LEP energies [10] but can be safely neglected at the scales considered here<sup>2</sup> and we will assume  $D_{i\neq Q_2}(z, \mu^2) = 0$  throughout.

## 2.4 SI Structure Functions at $\mathcal{O}(\alpha_s^1)$

In the next section we will consider three types of  $\mathcal{O}(\alpha_s^1)$  VFNS structure functions. The first two are constructed at full  $\mathcal{O}(\alpha_s^1)$

$$F_i^{QS^{(0+1)}+GF} - F_i^{SUB_q+SUB_g+[SUB_D]} \quad , \quad (18)$$

where the inclusion or omission of the bracketed  $SUB_D$  term corresponds to a running or scale-independent fragmentation function, respectively, as discussed in the previous section. It is somewhat unclear whether  $QS^{(1)}$  contributions (and the corresponding subtractions) should be considered on the same perturbative level as  $GF^{(1)}$ , see [1] for a more detailed discussion on that point. In the original formulation of the ACOT scheme [14]  $QS^{(1)}$  contributions are neglected at the level we are considering here and we therefore do also consider this option via the partial  $\mathcal{O}(\alpha_s^1)$  structure function

$$F_i^{QS^{(0)}+GF} - F_i^{SUB_g} \quad . \quad (19)$$

For obtaining the numerical results of the next section the general formulae of this section have to be adjusted by choosing masses and couplings according to the relevant NC and CC values as listed in [1]. For the CC case where  $Q_1$  should be identified with strange

---

<sup>2</sup> We could therefore, in principle, restrict the evolution of the charm FF to the nonsinglet sector.

quarks the boundary condition in Eq. (16) is inadequate since  $m_s^2 \sim \Lambda_{QCD}^2$  is below the perturbative regime of QCD. We will have recourse to standard strange seas from the literature [27, 28] instead.

### 3 The Charm Fragmentation Function in SI DIS

We will investigate the charm fragmentation function in CC and in NC SI DIS. In CC DIS the charm production mechanism is undebated since charm is dominantly produced by scattering on light strange quanta. Our reasoning will therefore be that  $D_c$  is directly accessible in CC DIS at relatively low spacelike momentum transfer. An extracted  $D_c$  can then be applied to NC DIS, where it might give insight into the details of the production dynamics [2]. Also a test of the universality [29] of the charm FF measured in CC DIS and  $e^+e^-$  annihilation [10] would be an important issue directly related to the factorization theorems [30] of perturbative QCD (pQCD).

All  $\varepsilon_c$  parameters discussed below refer to a Peterson type [23] functional form given by

$$D_c(z) = N \left\{ z \left[ 1 - z^{-1} - \varepsilon_c / (1 - z) \right]^2 \right\}^{-1} \quad (20)$$

where  $N$  normalizes  $D_c$  to  $\int dz D_c(z) = 1$ .

#### 3.1 CC DIS

In CC DIS one does not expect to gain much insight into the charm production process since charm is dominantly produced in scattering events on strange quarks<sup>3</sup> in the nucleon, thereby permitting an experimental determination of the strange quark content of the nucleon [5, 6, 7]. On the other hand the well understood production mechanism makes a direct determination of the charm fragmentation function feasible by measuring the

---

<sup>3</sup> We assume a vanishing Cabibbo angle. Our results remain, however, unchanged if the  $CKM$  suppressed  $d \rightarrow c$  background is included.

energy spectrum of final state charm fragments. This is obvious in leading order accuracy where<sup>4</sup>

$$d\sigma_{LO} \propto s(\chi) D_c(z) \quad (21)$$

is directly proportional to  $D_c$ . More precisely, it is not  $z$  but the closely related energy of the  $c \rightarrow \mu\nu$  decay muon which can be observed in iron detectors [5, 6, 7]. The smearing effects of the decay complicates the determination of the precise shape of  $D_c$  but only weakly influences an extraction of  $\langle z \rangle$  [5] which is valuable information if physically motivated one-parametric ansätze [23, 31] for  $D_c$  are *assumed*. At NLO the production cross section is no longer of the simple factorized form of Eq. (21) [12] and double convolutions (symbol  $\otimes$  below) of the form of Eqs. (7), (11) have to be considered. However, to a reasonable approximation

$$\begin{aligned} d\sigma_{NLO} &= ([s \otimes d\hat{\sigma}_s + g \otimes d\hat{\sigma}_g] \otimes D_c)(x, z, Q^2) \\ &\equiv d\sigma_{LO} K(x, z, Q^2) \\ &\propto s(\chi) D_c(z) K(x, z, Q^2) \\ &\simeq s(\chi) \mathcal{D}_{x, Q^2}[D_c](z) \end{aligned} \quad (22)$$

holds also at NLO accuracy within experimental errors and for the limited kinematical range of present data on neutrino production of charm. In Eq. (22) the approximate multiplicative factor  $\mathcal{D}$  absorbs the precise  $K$ -factor  $K(x, z, Q^2)$  obtained from a full NLO QCD calculation [12].  $\mathcal{D}$  is *not* a simple universal fragmentation function but a nontrivial process-dependent functional which is, however, mainly sensitive on  $D_c$  and shows little sensitivity on the exact parton distributions considered. The occurrence of  $x, Q^2$  and  $z$  in Eq. (22) as indices and as a functional argument, respectively, reflects the fact that the dependence on  $x$  and  $Q^2$  is much weaker than is on  $z$ . Eq. (22) tells us that  $s(\chi)$  fixes the normalization of  $d\sigma$  once  $K$  is known. On the other hand  $K$  (or  $\mathcal{D}$ ) can be computed [12] from  $D_c$  with little sensitivity on  $s(\chi)$ , such that  $s(\chi)$  and  $D_c(z)$  decouple in the production dynamics and can be simultaneously extracted. This point can be clearly inferred from Fig. 1 where it is shown that the wide spread of CC charm produc-

---

<sup>4</sup> We will suppress some obvious scale-dependences in the following formulae and in their discussion.

tion predictions which were obtained in [12] using GRV94 [27] and CTEQ4 [28] strange seas can be brought into good agreement by a mere change of the normalization given by the ratio  $s_{GRV}(\chi)/s_{CTEQ4}(\chi)$ . The remaining difference is not within present experimental accuracy which can be inferred from the shaded band representing a parametrization [12] of CCFR data [6]. High statistics neutrino data therefore offer an ideal scenario to measure  $D_c$  complementary to an extraction from LEP data on  $e^+e^- \rightarrow DX$  [10, 24]. This has been first noted in [29] where also a successful test of the universality of the charm FF has been performed. With new data [5, 6, 7]<sup>5</sup> at hand and with a sounder theoretical understanding [12] of neutrino production of charm it would be desirable to update the analysis in [29]. Nowadays one can in principle examine the possibility of a uniform renormalization group transformation from spacelike momenta near above the charm mass ( $\nu N \rightarrow DX$ ) to timelike momenta at the  $Z^0$  peak ( $e^+e^- \rightarrow DX$ ). In [10, 24] charm fragmentation functions extracted from LEP data have been tested against  $p_T$  and  $\eta$  distributions measured in photoproduction at HERA. However, we believe that a comparison to  $z$  differential neutrino production data is worthwhile beyond, since the latter measure directly the fragmentation spectrum whereas  $p_T$  and  $\eta$  shapes are rather indirectly influenced by the precise hardness of the FF via their normalization [10, 11]. Unfortunately up to now no real production data are available but only strange sea extractions [5, 6, 7] resulting from an analysis of the former. We therefore strongly recommend that experiments publish real production data such that the above outlined program can be executed with rigour. Here we can only find a  $\varepsilon_c$  parameter which lies in the correct ball park and examine a few points which will become relevant for an extraction of  $D_c$  once data will become available.

An outstanding question is the possible effect of a finite strange mass on the full semi-inclusive charm production cross section [21] including  $\mathcal{O}(\alpha_s^1)$  quark scattering contributions. By comparing the thick and the thin solid curve in Fig. 2 (a) it is clear that the effect of a finite  $m_s$  can be neglected even at low scales and for a maximally reasonable

---

<sup>5</sup> Data from NuTeV [32] is to be expected in the near future;  $\mu^\pm$  events observed at NOMAD await further analysis [33].

value of  $m_s = 500$  MeV. For the larger scale of Fig. 2 (b) the effect of choosing a finite  $m_s$  would be completely invisible. A further question which might influence the extraction of a universal FF from neutrino production is the one of the scheme dependence in handling final state quasi-collinear logarithms  $\ln(Q^2/m_c^2)$ . If these are subtracted from the coefficient functions as discussed in section 2.3, the subtraction defines a running of the charm FF which becomes scale dependent<sup>6</sup> according to Eq. (17). In Fig. 2 we examine such resummation effects for CCFR kinematics [6]. We use the same Peterson FF with  $\varepsilon_c = 0.06$  [34, 12] once for a fixed order calculation [12] (solid lines) and once as the non-perturbative part on the right hand side of the entire  $c \rightarrow D$  FF on the left hand side of Eq. (17) (dashed curves). We note that towards intermediate scales around  $Q^2 \sim 20\text{GeV}^2$  one begins to see the softening effects of the resummation which are enhanced as compared to FOPT. However, as one would expect at these scales, the resummation effects are moderate and could be compensated by only a *slight* shift of the  $\varepsilon_c$  parameter which is therefore, within experimental accuracy, insensitive to scheme transformations. We note that – as was already shown in [12] – according to Fig. 1 an  $\varepsilon_c$  of around 0.06 which we took from an older analysis in [34] seems to reproduce the measured spectrum quite well. For  $\langle E_\nu \rangle = 80\text{GeV}$ ,  $\langle Q^2 \rangle = 20\text{GeV}^2$  a value  $\varepsilon_c \simeq 0.06$  gives an average  $\langle z \rangle \simeq 0.6$  consistent with  $\langle z \rangle = 0.68 \pm 0.08$  measured by CDHSW [5]. In [10]<sup>7</sup> a distinctly harder value of  $\varepsilon_c \simeq 0.02$  was extracted from LEP data on  $e^+e^- \rightarrow D^*X$ . If the latter fit is evolved down to fixed target scales it is – even within the limited experimental accuracy – incompatible with the CCFR neutrino data represented in Fig. 1. From Fig. 2 it is clear that the difference cannot be attributed to a scheme dependence of the  $\varepsilon_c$  parameter which is too small to explain the discrepancy. It would of course be interesting to know how much the above mentioned smearing effect of the  $c \rightarrow \mu\nu$  decay might dilute the discrepancy. In any case, charm fragmentation at LEP has been measured by tagging on  $D^*$ 's whereas neutrino production experiments observe mainly  $D$ 's through their semileptonic

---

<sup>6</sup> Evolving the charm FF we adopt for consistency the evolution parameters  $m_{c,b}$  and  $\Lambda_{4,5}^{QCD}$  of the CTEQ4(M) [28] parton distribution functions and we use  $\tilde{Q}_0 = m_c$ .

<sup>7</sup> The  $\varepsilon_c$  value in [24] has no connection to a massive calculation and cannot be compared to the values discussed here.

decay-channel (dimuon events). ARGUS [36] and CLEO [37] data at  $\sqrt{s} \simeq 10\text{GeV}$  indeed show [38] a harder energy distribution of  $D^*$ 's compared to  $D$ 's. It seems therefore to be possible within experimental accuracy to observe a nondegeneracy of the charm fragmentation functions into the lowest charmed pseudoscalar and vector mesons. We note that an  $\varepsilon_c$  value around 0.06 which is in agreement with neutrino data on  $D$ -production is also compatible with the  $D$  energy spectrum measured at ARGUS where the evolution may be performed either via FOPT using expressions in [9] or via a RG transformation along the lines of [19, 10]. If forthcoming experimental analyses should confirm our findings the lower decade  $m_c(\sim 1\text{GeV}) \rightarrow \text{ARGUS}(10\text{GeV})$  may be added to the evolution path  $\text{ARGUS}(10\text{GeV}) \rightarrow \text{LEP}(M_Z)$  paved in [10] for the charm FF.

### 3.2 NC DIS

The fragmentation function of charm quarks observed in NC DIS is of special interest since it allows for directly investigating [2, 3] the charm production mechanism which is a vividly discussed issue in pQCD phenomenology [25, 17, 39]. Whereas for intrinsic heavy quarks one expects to observe a Peterson-like hard spectrum attributed to the dominance of the leading order quark scattering contribution, one expects a much softer spectrum for extrinsic GF since the gluon radiates the  $c\bar{c}$  pair towards lower energies ( $z$ ) during the hard production process before the nonperturbative hadronization takes place. Experimental analyses have been performed in [2, 3] and the steep spectrum<sup>8</sup> (best visible in Fig. 6 in [2]) of observed  $D$ -mesons together with the missing of a hard component at larger  $z$  seem to give clear evidence for the dominance of extrinsic  $GF$  over  $QS$  which was excluded at the 5% level [2]. In a complete VFNS the  $QS^{(0)}$  component makes, however, just one part of the  $\mathcal{O}(\alpha_s^1)$  structure functions in Eqs. (18), (19). Especially, there also exists a  $GF^{(1)}$  component, albeit with the leading log part of it subtracted. Since the subtraction term in Eq. (13) is proportional to  $D_c$  and therefore only removes a hard component from  $GF^{(1)}$  one expects the rise towards lower  $z$  to survive the subtraction. Furthermore a perturba-

---

<sup>8</sup> The variable  $x_D$  considered in [2, 3] differs slightly from  $z$  in definition. The variables are, however, identical at the 2% level [40].

tive evolution of the charm fragmentation function  $D_c(z, Q^2)$  might soften somewhat the hard QS term.

These expectations can be quantitatively confirmed in Fig. 3 where we show for HERA kinematics [2] the total (solid line) normalized  $\mathcal{O}(\alpha_s^1)$  production cross section for transverse virtual photons ( $F_L = 0$ ) on protons. We also show the individual components contributing to it: The processes  $\gamma^* g \rightarrow c\bar{c}$  (dot-dashed) and  $\gamma^* c \rightarrow cg$  (dotted; incl. virtual corrections) correspond to the  $GF^{(1)} - SUB_g$  and  $QS^{(1)} - SUB_q - SUB_D$  terms, respectively, subtracted at  $\mu = Q$ . They are *not* physically observable and only sensible if they are added to the  $QS^{(0)}$  Born term (dashed) as in Eqs. (18), (19). We have perturbatively resummed all logarithms of the charm mass via massless evolution equations starting at the charm mass [ $Q_0 = \tilde{Q}_0 = m_c$ ] and using the standard boundary conditions in Eqs. (16), (17) for  $\varepsilon_c = 0.06$ . Finite charm mass effects on the subtracted  $QS^{(1)}$  contribution can be inferred by comparing the thick and the thin dotted curves, where the  $m_c \rightarrow 0$  limit has been taken for the latter. As has been theoretically anticipated in [35] the charm mass can be safely set to zero in  $QS^{(1)}$  and the involved convolutions in Eq. (5) may be replaced by the massless expressions in [8, 22] which simplifies the numerics essentially and which we will therefore do for the  $\mu = 2m_c$  curve in Fig. 4 below. As also stressed in [35] it is, however, essential to keep the charm mass finite in the  $GF^{(1)}$  contribution since  $m_c$  tempers the strength of the  $z'^{-1} \hat{u}$ -channel propagator singularity. Obviously the  $\mathcal{O}(\alpha_s^1)$  result of an ACOT based calculation deviates essentially from the naive Born term expectation and it seems by no means legitimate to treat  $GF^{(1)}$  as a higher order correction here. Contrary to the corresponding inclusive results in [1] and to the expectations in [14] also the subtracted  $QS^{(1)}$  term is numerically significant in the semi-inclusive case considered here. In the light of the huge  $\mathcal{O}(\alpha_s^1)$  corrections it seems, however, undecidable as to whether include or omit  $QS^{(1)}$  at  $\mathcal{O}(\alpha_s^1)$  without knowing  $\mathcal{O}(\alpha_s^2)$  corrections within ACOT.

In Fig. 4 the resummed result (VFNS: solid lines) can be compared to unsubtracted



$\mathcal{O}(\alpha_s^1)^9$   $GF^{(1)}$  (fixed order, dashed line). We show the total  $\mathcal{O}(\alpha_s^1)$  VFNS result for the choices  $\mu = Q, 2m_c$ . The modest scale dependence arises exclusively through the  $QS^{(1)}$  term. For any of the other curves a variation of  $\mu$  is completely insignificant and we therefore only show  $\mu = Q$ . A full VFNS calculation (solid lines) seems hardly distinguishable from fixed order perturbation theory (dashed line) within experimental accuracy. The two approaches are even closer if one follows the suggestion in [14] and does not include (dot-dashed line) the subtracted  $QS^{(1)}$  term at the level of  $QS^{(0)} + GF^{(1)}$ . The data points in the figure correspond to H1 measurements [2] of  $D^0$  (circles) and  $D^{*+}$  (triangles; both including charge conjugation) spectra. The measurement is restricted to  $\eta_D < 1.5$ . Extrapolating to the full phase space gives rise to large acceptance corrections which are, however, quite uniform [40] over the kinematical range considered and therefore have a minor effect on the *normalized* spectrum. Since FOPT and ACOT based calculations are very close it seems improbable that an experimental discrimination between the two approaches will be possible. The born term in Fig. 3 is far from being the dominant contribution and an intrinsic  $c(x, Q^2)$  stemming from the resummation of perturbative logs can therefore not be excluded. The tendency of the data appears somewhat softer than any of the calculations and the tendency seems to be confirmed by preliminary data in a lower  $z$  bin [42]. The resummed calculation appears to be too hard at larger  $z$  around 0.6 if the  $QS^{(1)}$  component is included. As already mentioned, at the present stage of the calculations it can not be decided whether this hints at an intrinsic problem within VFNS calculations or whether this may be cured by  $\mathcal{O}(\alpha_s^2)$  corrections.

## 4 Conclusions

In this paper we have performed an ACOT [14] based analysis of heavy quark fragmentation in DIS including a calculation of semi-inclusive scattering on massive quarks at  $\mathcal{O}(\alpha_s^1)$  for general masses and couplings. As in the inclusive case [1] effects from finite initial state quark masses can be neglected for practical applications to charm production in CC

---

<sup>9</sup> An  $\mathcal{O}(\alpha_s^2)$  NLO calculation [41] within FOPT gives very similar results [40].

and NC DIS. The involved convolutions in section 2.1 can therefore safely be replaced by their analogues in [8, 22, 12]. Neutrinoproduction is an ideal environment to extract the charm FF within DIS and a Peterson [23] type FF with  $\varepsilon_c \simeq 0.06$  seems to lie in the correct ball park, where the sensitivity on the choice of scheme is small and finite  $m_s$  effects are irrelevant. The  $\varepsilon_c$  value above is compatible with  $e^+e^-$  data if a nondegeneracy of charm quarks fragmenting into  $D$ 's and  $D^*$ 's is allowed for. For NC DIS it seems unlikely that a discrimination between fixed order and resummed calculations will be possible at HERA. Both approaches give similar results which show a spectrum that is somewhat harder than the tendency of the data [2, 3, 42]. The resummed calculation is made worse if the  $\mathcal{O}(\alpha_s^1)$  quark scattering contribution is included at the perturbative level considered in this paper.

## Acknowledgements

We thank E. Reya for advice, useful discussions and a careful reading of the manuscript and K. Daum for several helpful correspondences on the HERA analyses. This work has been supported in part by the 'Bundesministerium für Bildung, Wissenschaft, Forschung und Technologie', Bonn.

## Appendix A: Matrix Elements for Real Gluon Emission

The projections  $\hat{f}_i^Q$  of the partonic Matrix Element onto the structure functions are most conveniently given in the Mandelstam variables  $\hat{s}_1$  and  $\hat{t}_1$  which are defined below Eq. (10):

$$\begin{aligned}
\hat{f}_1^Q(\hat{s}_1, \hat{t}_1) &= \frac{8}{\Delta'^2} \left\{ -\Delta^2(S_+\Sigma_{++} - 2m_1m_2S_-) \left( \frac{m_2^2}{\hat{s}_1^2} + \frac{m_1^2}{\hat{t}_1^2} + \frac{\Sigma_{++}}{\hat{s}_1\hat{t}_1} \right) \right. \\
&+ 2m_1m_2S_- \left( \frac{m_1^2\hat{s}_1(\hat{s}_1 + 2\Sigma_{+-})}{\hat{t}_1^2} + \frac{\Delta'^2 + (m_2^2 + Q^2)\hat{s}_1 + 2\Sigma_{+-}\Sigma_{++}}{\hat{t}_1} \right. \\
&+ \frac{\Delta'^2 - \hat{s}_1(m_1^2 + Q^2 + \hat{s}_1) + 2m_2^2\Sigma_{+-}}{\hat{s}_1} - \hat{t}_1 \frac{(m_2^2 + \hat{s}_1)}{\hat{s}_1} \Big) \\
&+ S_+ \left( -\frac{m_1^2\hat{s}_1\Sigma_{+-}(\hat{s}_1 + 2\Sigma_{++})}{\hat{t}_1^2} + \frac{-\hat{s}_1^3 - 4\hat{s}_1^2\Sigma_{+-} + \hat{s}_1(4m_1^2m_2^2 - 7\Sigma_{+-}\Sigma_{++})}{2\hat{t}_1} \right. \\
&+ \frac{2\Sigma_{++}(-\Delta^2 - 2\Sigma_{+-}\Sigma_{++})}{2\hat{t}_1} + \left[ 4m_1^4 + 2m_1^2\hat{s}_1 - \Sigma_{+-}(m_2^2 + \Sigma_{+-}) \right. \\
&- \left. \left. \frac{(\Delta^2 + 2m_2^2\Sigma_{+-})\Sigma_{++}}{\hat{s}_1} \right] - \hat{t}_1 \frac{\Delta'^2 - 2(m_2^2 + \hat{s}_1)\Sigma_{++}}{2\hat{s}_1} \Big) \right\} \\
\hat{f}_2^Q(\hat{s}_1, \hat{t}_1) &= \frac{16}{\Delta'^4} \left\{ -2\Delta^4S_+ \left( \frac{m_2^2}{\hat{s}_1^2} + \frac{m_1^2}{\hat{t}_1^2} + \frac{\Sigma_{++}}{\hat{s}_1\hat{t}_1} \right) + 2m_1m_2S_- \left( \frac{(\Delta'^2 - 6m_1^2Q^2)\hat{s}_1}{\hat{t}_1} \right. \right. \\
&+ \left[ 2(\Delta'^2 - 3Q^2(\hat{s}_1 + \Sigma_{++})) \right] + \hat{t}_1 \frac{\Delta'^2 - 6Q^2(m_2^2 + \hat{s}_1)}{\hat{s}_1} \Big) \\
&+ S_+ \left( \frac{-2m_1^2\hat{s}_1[(\Delta^2 - 6m_1^2Q^2)\hat{s}_1 + 2\Delta^2\Sigma_{+-}]}{\hat{t}_1^2} + \frac{-2\Delta^2(\Delta^2 + 2\Sigma_{+-}\Sigma_{++})}{\hat{t}_1} \right. \\
&+ \frac{-\hat{s}_1[2(\Delta^2 - 6m_1^2Q^2)\hat{s}_1 + (\Delta'^2 - 18m_1^2Q^2)\Sigma_{++} + 2\Delta^2(3\Sigma_{++} - 4m_1^2)]}{\hat{t}_1} \\
&+ \left[ -2(m_1^2 + m_2^2)\hat{s}_1^2 - 9m_2^2\Sigma_{+-}^2 - \frac{2\Delta^2(\Delta^2 + 2m_2^2\Sigma_{+-})}{\hat{s}_1} + 2\hat{s}_1[2\Delta^2 \right. \\
&+ \left. (m_1^2 - 5m_2^2)\Sigma_{+-}] + \Delta^2(2\Sigma_{++} - m_2^2) \right] - \hat{t}_1 \frac{[\Delta'^2 - 6Q^2(m_2^2 + \hat{s}_1)]\Sigma_{++}}{\hat{s}_1} \Big) \right\} \\
\hat{f}_3^Q(\hat{s}_1, \hat{t}_1) &= \frac{16}{\Delta'^2} \left\{ -2\Delta^2R_+ \left( \frac{m_2^2}{\hat{s}_1^2} + \frac{m_1^2}{\hat{t}_1^2} + \frac{\Sigma_{++}}{\hat{s}_1\hat{t}_1} \right) + 2m_1m_2R_- \left( \frac{\hat{s}_1 + \Sigma_{+-}}{\hat{t}_1} + \frac{\hat{s}_1 - \Sigma_{+-}}{\hat{s}_1} \right) \right. \\
&+ R_+ \left( \frac{-2m_1^2\hat{s}_1\Sigma_{+-}}{\hat{t}_1^2} + \frac{-\hat{s}_1^2 - 4(\Delta^2 - m_1^2\Sigma_{+-}) - 3\hat{s}_1\Sigma_{+-}}{\hat{t}_1} \right.
\end{aligned}$$

$$+ \left[ 2(m_1^2 - m_2^2) - \frac{2(\Delta^2 + m_2^2 \Sigma_{+-})}{\hat{s}_1} + \hat{t}_1 \frac{\hat{s}_1 - \Sigma_{-+}}{\hat{s}_1} \right) \Big\} \quad (\text{A1})$$

where we conveniently use the shorthands  $\Delta \equiv \Delta[m_1^2, m_2^2, -Q^2]$  and  $\Delta' \equiv \Delta[m_1^2, \hat{s}, -Q^2]$ . In order to obtain the inclusive results  $\hat{f}_i^Q(\hat{s}_1)$  in Appendix C of [1] the  $\hat{f}_i^Q(\hat{s}_1, \hat{t}_1)$  have to be integrated over  $0 \leq y \leq 1$ , i.e.

$$\hat{f}_i^Q(\hat{s}_1) = \int_0^1 dy \hat{f}_i^Q(\hat{s}_1, \hat{t}_1) \quad , \quad (\text{A2})$$

where  $y$  is defined via the the partonic center of mass scattering angle  $\theta^*$  and related to  $\hat{t}_1$  through

$$\begin{aligned} y &\equiv \frac{1}{2} (1 + \cos \theta^*) \\ \hat{t}_1 &= \frac{\hat{s}_1}{\hat{s}_1 + m_2^2} \Delta' (y - y_0) \quad , \end{aligned} \quad (\text{A3})$$

with  $y_0 = [1 + (\Sigma_{++} + \hat{s}_1)/\Delta']/2$  being the would-be collinear pole of the  $\hat{t}$ -channel propagator.

## References

- [1] S. Kretzer and I. Schienbein, **hep-ph 9709442**, to appear in Phys. Rev. **D**.
- [2] C. Adloff *et al.*, H1 collab., Z. Phys. **C72**, 593 (1996).
- [3] J. Breitweg *et al.*, ZEUS collab., Phys. Lett. **B407**, 402 (1997).
- [4] W. G. Seligman *et al.*, Phys. Rev. Lett. **79**, 1213 (1997);  
W. G. Seligman, Ph. D. thesis, Columbia University, Nevis-292 (1997).
- [5] H. Abramowicz *et al.*, CDHSW collab., C. Phys. **C15**, 19 (1982).
- [6] S. A. Rabinowitz *et al.*, CCFR collab., Phys. Rev. Lett. **70**, 134 (1993).
- [7] A. O. Bazarko *et al.*, CCFR collab., Z. Phys. **C65**, 189 (1995);  
A. O. Bazarko, Ph. D. thesis, Columbia University, Nevis-285 (1994).
- [8] G. Altarelli, R. K. Ellis, G. Martinelli and S.-Y. Pi, Nucl. Phys. **B160**, 301 (1979).
- [9] P. Nason and B. R. Webber, Nucl. Phys. **B421**, 473 (1994); Erratum **480**, 755 (1996).
- [10] M. Cacciari and M. Greco, Phys. Rev. **D55**, 7126 (1997).
- [11] J. Breitweg *et al.*, ZEUS collab., DESY 98-085, **hep-ex 9807008**.
- [12] M. Glück, S. Kretzer and E. Reya, Phys. Lett. **B398**, 381 (1997); Erratum **B405**, 392 (1997).
- [13] S. J. Brodsky, P. Hoyer, C. Peterson and N. Sakai, Phys. Lett. **B93**, 451 (1980);  
S. J. Brodsky, C. Peterson and N. Sakai, Phys. Rev. **D23**, 2745 (1981).
- [14] M. A. G. Aivazis, J. C. Collins, F. I. Olness and W.-K. Tung, Phys. Rev. **D50**, 3102 (1994).
- [15] R. S. Thorne and R. G. Roberts, Phys. Rev. **D57**, 6871 (1998) ;  
R. S. Thorne and R. G. Roberts, Phys. Lett. **B421**, 303 (1998).

- [16] A. D. Martin, R. G. Roberts, M. G. Ryskin and W. J. Stirling, Eur. Phys. J. **C2**, 287 (1998).
- [17] M. Buza, Y. Matiounine, J. Smith, W. L. van Neerven, Eur. Phys. J. **C1**, 301 (1998).
- [18] J. C. Collins and W.- K. Tung, Nucl. Phys. **B278**, 934 (1986); S. Qian, Argonne preprint ANL-HEP-PR-84-72, (*unpublished*).
- [19] B. Mele and P. Nason, Nucl. Phys. **B361**, 626 (1991).
- [20] M. A. G. Aivazis, F. I. Olness and W.- K. Tung, Phys. Rev. **D50**, 3085 (1994).
- [21] S. Kretzer and I. Schienbein, Phys. Rev. **D56**, 1804 (1997).
- [22] W. Furmanski and R. Petronzio, Z. Phys. **C11**, 293 (1982).
- [23] C. Peterson et al., Phys. Rev. **D27**, 105 (1983).
- [24] J. Binnewies, B. A. Kniehl and G. Kramer, Phys. Rev. **D58**, 014014 (1998).
- [25] M. Glück, E. Reya and M. Stratmann, Nucl. Phys. **B422**, 37 (1994).
- [26] K. G. Chetyrkin, B. A. Kniehl and M. Steinhauser, Phys. Rev. Lett. **79**, 2184 (1997).  
W. Wetzel, Nucl. Phys. **B196**, 259 (1982); W. Bernreuther and W. Wetzel, Nucl. Phys. **B197**, 228 (1982); W. Bernreuther, Ann. Phys. **151**, 127 (1983); W. Bernreuther, Z. Phys. **C20**, 331 (1983); S. A. Larin, T. van Ritbergen and J. A. M. Vermaseren, Nucl. Phys. **B438**, 278 (1995).
- [27] M. Glück, E. Reya and A. Vogt, Z. Phys. **C67**, 433 (1995).
- [28] H. L. Lai *et al.*, CTEQ collab., Phys. Rev. **D55**, 1280 (1997).
- [29] K. Kleinknecht and B. Renk, Z. Phys. **C17**, 325 (1983).
- [30] J. C. Collins, D. Soper and G. Sterman, in A. H. Mueller, ed., *Perturbative Quantum Chromodynamics* (World Scientific 1989).
- [31] P. Collins and T. Spiller, J Phys. **G11**, 1289 (1985).

- [32] J. Yu, talks given at the *33rd Rencontres de Moriond: QCD and High Energy Hadronic Interactions*, Les Arcs, March 1998; *6th International Workshop on Deep Inelastic Scattering and QCD (DIS98)*, Brussels, April 1998.
- [33] K. Zuber, private communication.
- [34] J. Chrin, Z. Phys. **C36**, 163 (1987).
- [35] J. C. Collins, PSU-TH/198, hep-ph 9806259.
- [36] H. Albrecht *et al.*, ARGUS collab., Z. Phys. **C52**, 353 (1991).
- [37] D. Bortoletto *et al.*, CLEO collab., Phys. Rev. **D37**, 1719 (1988).
- [38] This point is well illustrated in Fig. 36.13 in the 1996 *Review of particle Physics*, R. M. Barnett *et al.*, Phys. Rev. **D54**, 1 (1996).
- [39] F. I. Olness and S. T. Riemersma, Phys. Rev. **D51**, 4746 (1995);  
H. L. Lai and W.-K. Tung, Z. Phys. **C74**, 463 (1997);  
E. Laenen *et al.*, proceedings of the workshop *Future Physics at HERA*, eds. G. Ingelman, A. De Roeck and R. Klanner, Hamburg 1996.
- [40] K. Daum, private communication.
- [41] B. W. Harris and J. Smith, Nucl. Phys. **B452**, 109 (1995).
- [42] K. Tzamariudaki, talk given at the *29th International Conference on High-Energy Physics ICHEP 98*, Vancouver, July 1998.

## Figure Captions

**Fig. 1** The charm production cross section obtained in [12] for two  $x, Q^2$  points in the CCFR [6] kinematical regime. Up to a constant of normalization which was conveniently chosen in Eq. (4) of [12]  $s_{eff}$  represents the triple differential cross section  $d^3\sigma/dxdydz$  where  $x$  and  $y$  are standard and  $z \equiv p_D \cdot p_N / q \cdot p_N$ . Shown are the predictions using GRV94 [27] (solid) and CTEQ4 [28] (dashed) partons and a curve (dot-dashed) where the normalization of the CTEQ4 prediction is changed by multiplying with the ratio of the strange seas  $s_{GRV}(\chi)/s_{CTEQ}(\chi)$ . For all curves a scale-independent Peterson FF with  $\varepsilon_c = 0.06$  has been used.

**Fig. 2** The same quantity as in Fig. 1. All predictions have been obtained for the CTEQ4 parton distributions. The solid curves result from a scale-independent Peterson FF with  $\varepsilon_c = 0.06$ . In (a) the thin solid curve has been obtained using the formulae of section 2 and choosing a finite strange quark mass of  $m_s = 500\text{MeV}$  whereas the thicker curve corresponds to the asymptotic  $m_s \rightarrow 0$  limit ( $\equiv \overline{\text{MS}}$ ). In (b) these two options would be completely indistinguishable and we only show the  $\overline{\text{MS}}$  result. For the dot-dashed curves the final state quasi-collinear logarithm has been absorbed into a running of the charm FF. A Peterson FF with  $\varepsilon_c = 0.06$  has been used as the nonperturbative part of the input as given in Eq. (17).

**Fig. 3** The normalized charm production cross section  $d\sigma/dz$  ( $z \equiv p_D \cdot p_N / q \cdot p_N$ ) for HERA kinematics ( $\sqrt{s} = 314\text{GeV}$ ). For a comparison with H1 data [2] the cross section has been integrated over  $10\text{GeV}^2 < Q^2 < 100\text{GeV}^2$  and  $0.01 < y < 0.7$ . Following the experimental analysis [2] only contributions from transverse photons ( $F_L = 0$ ) are considered. Shown is the total  $\mathcal{O}(\alpha_s^1)$  result (solid line) and the individual contributions. Details to the calculation of the total result and the individual contributions are given in the text. The charm mass has been kept finite at the CTEQ4 value of  $m_c = 1.6\text{GeV}$  everywhere except for the thin dotted curve where the  $m_c \rightarrow 0$  limit has been taken.



**Fig. 4** A Comparison of the total  $\mathcal{O}(\alpha_s^1)$  result (solid lines) to H1 data [2] on  $D^0$  (circles) and  $D^{+*}$  (triangles; both including charge conjugation) production. Shown are results for two choices of the factorization/renormalization scale  $\mu$ . Also shown is the outcome of a fixed order  $\mathcal{O}(\alpha_s^1)$   $GF$  calculation for comparison (dashed line). The dot-dashed line follows the suggestion in [14] and neglects quark initiated contributions at  $\mathcal{O}(\alpha_s^1)$ , i.e. the difference between the solid ( $\mu = Q$ ) and the dot-dashed line is given by the (thick) dotted line in Fig. 3. For the dot-dashed curve as well as for the fixed order calculation (dashed) only  $\mu = Q$  is shown since the scale dependence is completely insignificant.

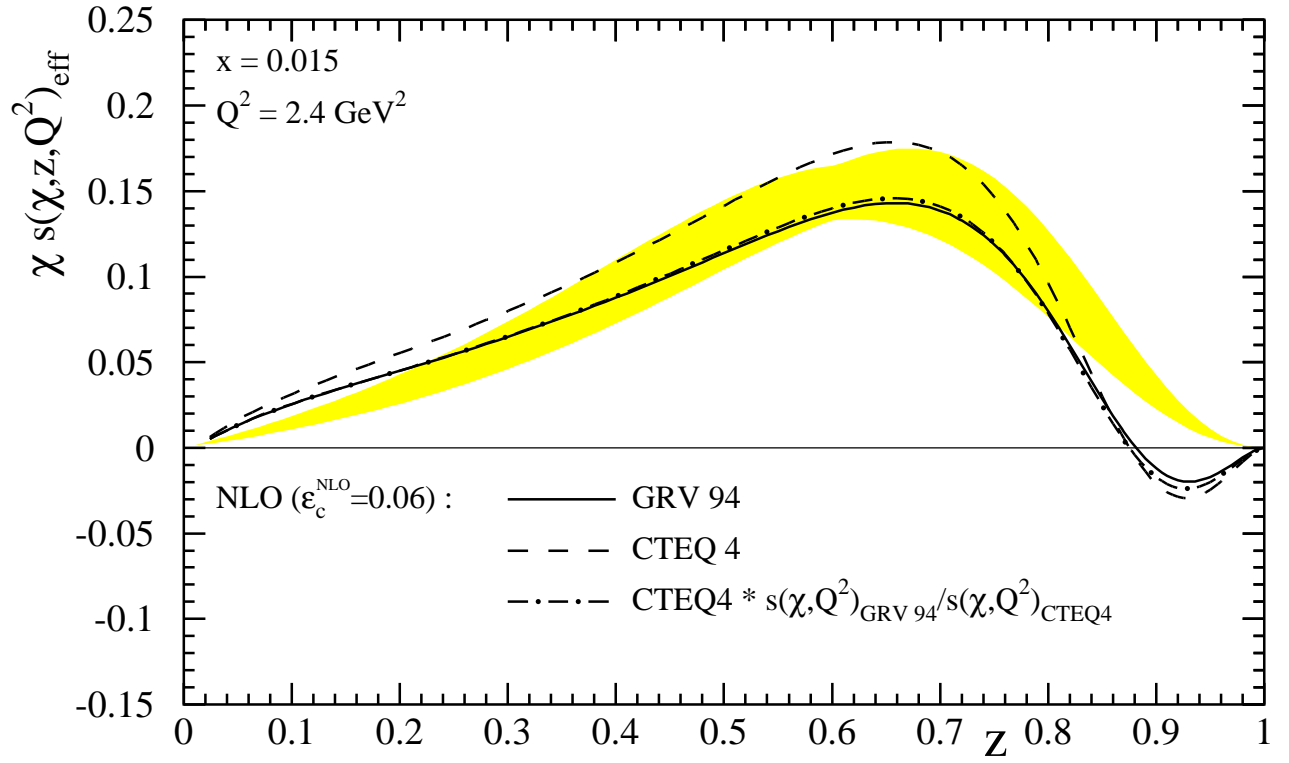


Fig. 1 (a)

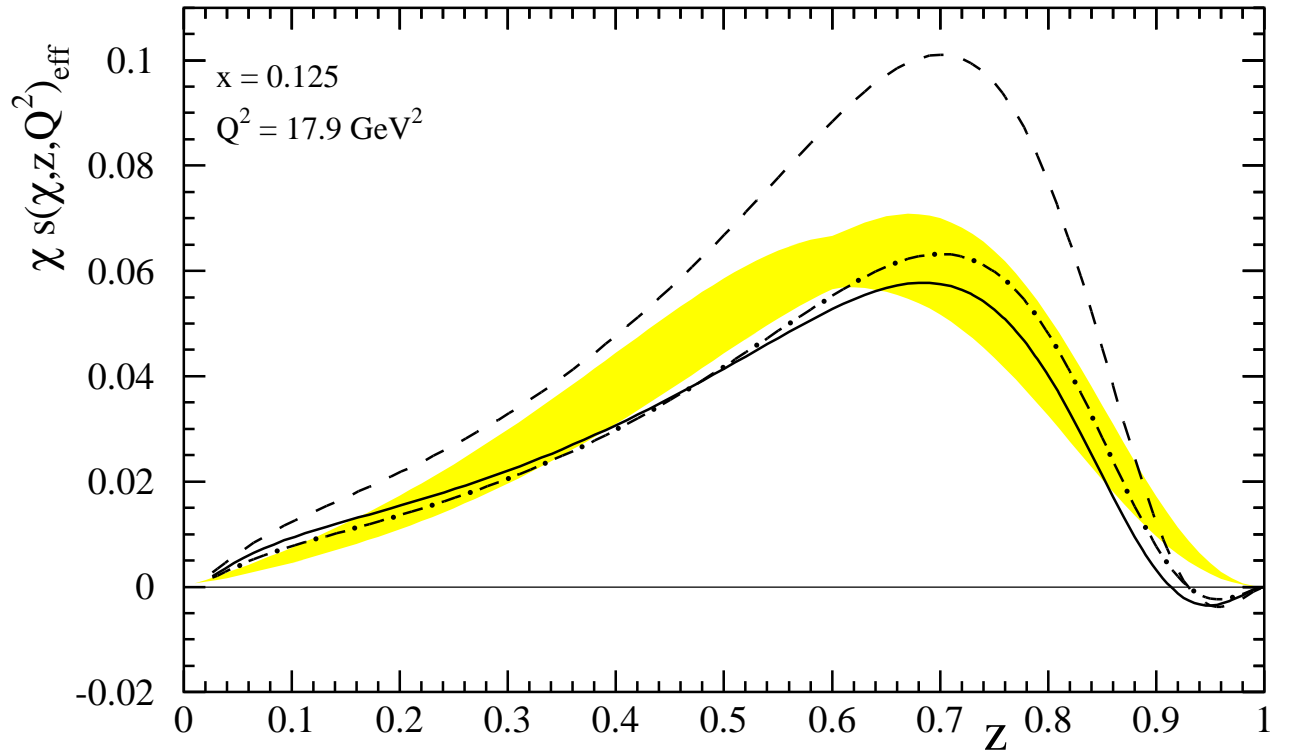


Fig. 1 (b)

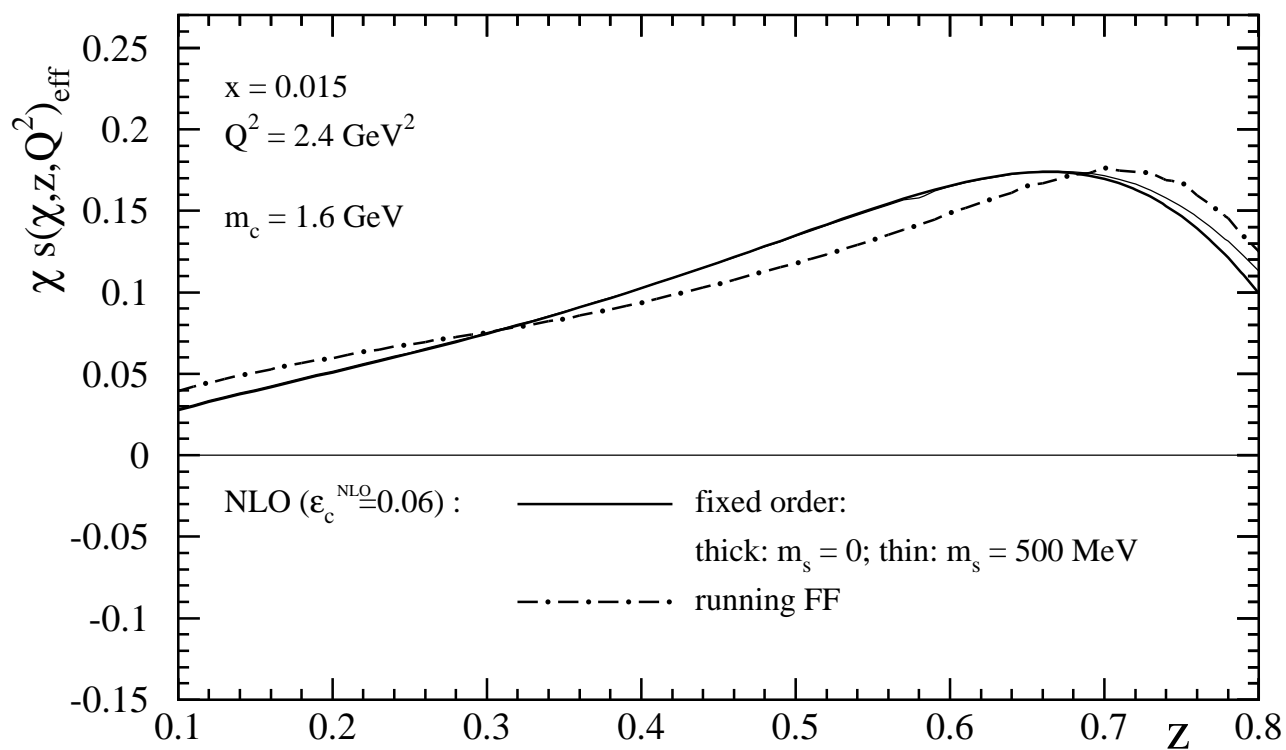


Fig. 2 (a)

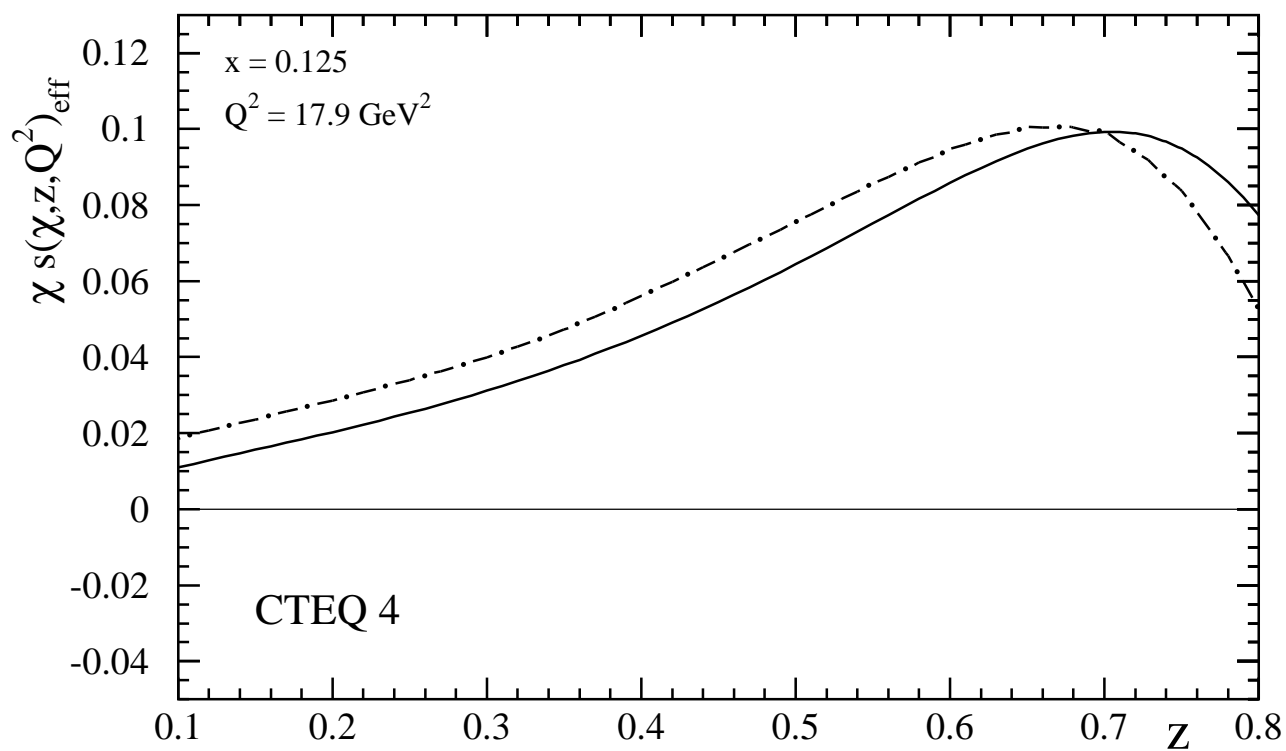


Fig. 2 (b)

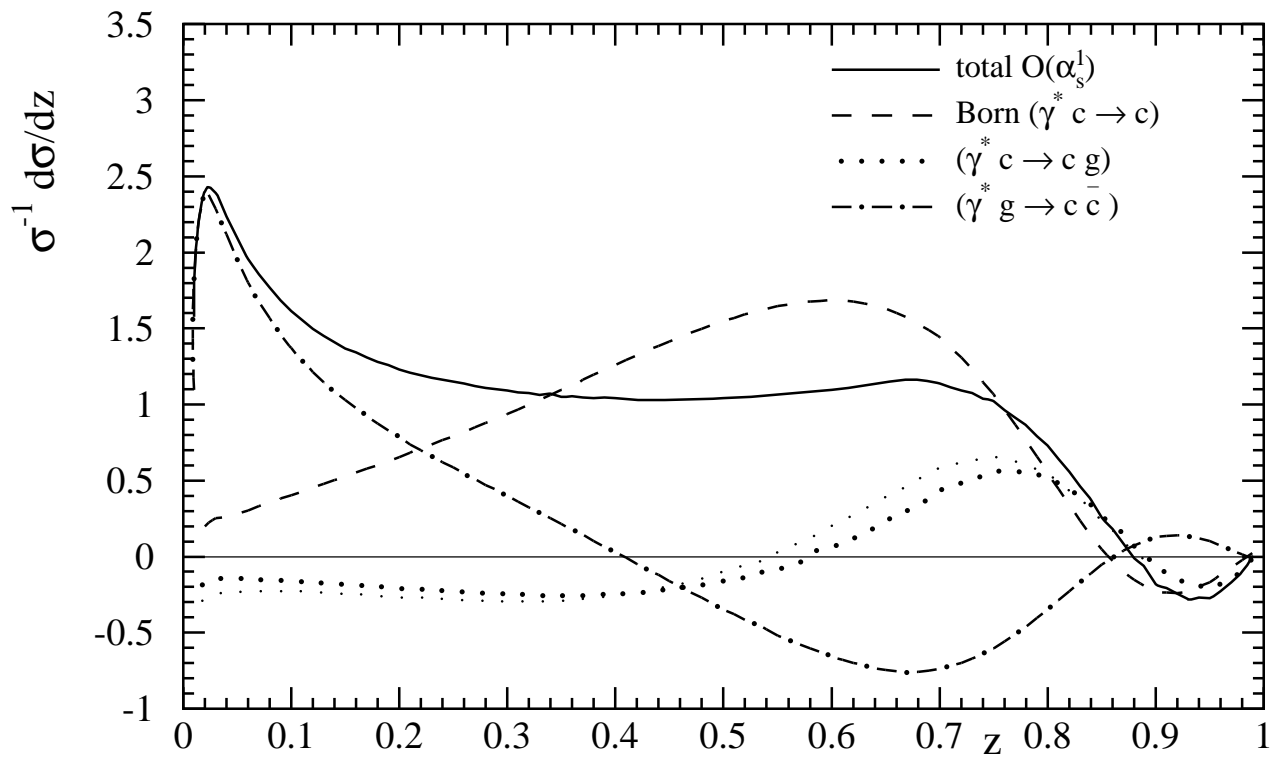


Fig. 3

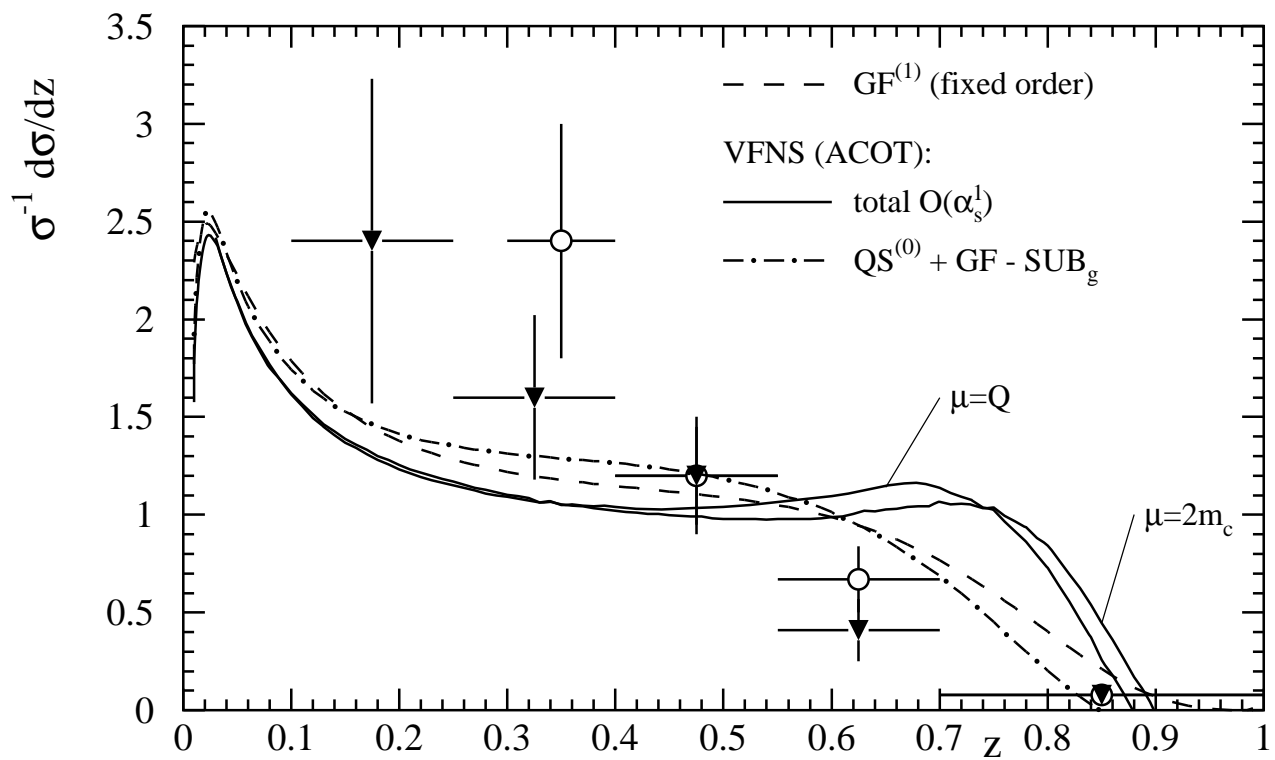


Fig. 4